moment has been eliminated by use of the distributed origin gauge. However, the basis set, though large, does not have the extensive polarization which Stephens' investigations on NHDT[30,31] suggest is necessary for converged results. On the other hand, the present results were obtained with a very large (equivalent in size to 6-311G**), properly derivatized, basis set, but were evaluated in the common origin gauge (center of mass) and are origin dependent. The agreement between calculated and experimental spectra suggests that the present results are not far from the correct values. More comparisons are necessary before one could conclude that the center of mass is a reasonable choice of origin and/or that the origin dependence is not severe with the 6-31G~ basis set.

(31) (a) Jalkanen, K. J.; Stephens, P. J.; Lazzeretti, P.; Zanasi, R. *J. Chem. Phys.* **1989**, *90*, 3204-3213. (b) Jalkanen, K. J.; Stephens, P. J.; Amos, R. D.; Handy, N. C. *Chem. Phys. Lett.* **1987**, *142*, 153-158.

Acknowledgment. The authors are grateful to Professors H. S. Mosher and T. Cronholm who kindly provided samples of optically active α-*d*-ethanol from which the measured VCD spectra were obtained. The financial support of the Natural Sciences and Engineering Research Council of Canada is gratefully acknowledged. We also thank Supercomputer Services of the University of Calgary for generous allocations of CPU time on the CDC Cyber 205.

Theoretical Study of Ethylene–Noble Metal Complexes

G. Nicolas* and F. Spiegelmann

Contribution from the Laboratoire de Physique Quantique, U.A. 505 du CNRS Université Paul Sabatier, 118, Route de Narbonne, 31062 Toulouse Cedex, France. *Received July 14, 1989*

Abstract: The interaction of ethylene with copper, silver, or gold atoms is investigated through theoretical calculations, including electron correlation effects. The $d^{10}s^1$ atomic configuration of the three metals gives rise to a weakly bound $^2A_1$ ground state (D_e < 12 kcal·mol^{-1}) in which the interaction is analyzed as a van der Waals one. The $^2B_1$ and $^2B_2$ states arising from the $d^{10}p^1$ atomic configurations give more bound complexes (D_e > 20 kcal·mol^{-1}). Gold is found to have the highest complexing ability, while silver yields the less bound complexes. The calculated vertical transitions are in good agreement with the observed UV-visible spectrum of CuC_2H_4 and AuC_2H_4. These transitions are related to s → p excitations of the metal unpaired electron.

I. Introduction

In recent years, low-temperature cocondensation of metal atoms with alkenes[1] or alkynes[2] in rare-gas matrices has provided various spectroscopic data such as infrared (IR) and Raman vibrationnal spectra,[3,4] UV-visible absorption spectra,[5-9] and electron spin resonance (ESR) studies.[10-14]

This is the case for copper, silver, and gold metal atoms M, which have been observed to react with ethylene and form $M_n(C_2H_4)_m$ complexes. However, the numerous experimental data available on this series reveal some contradictions. Indeed, the ESR experiments of Kasai et al.[15,16] give evidence for the biligand $M(C_2H_4)_2$ complexes with the three metals, while the monoligand MC_2H_4 π-type complexes are observed only with copper and gold but not with silver. The IR and UV-visible experiments of McIntosh et al.[17] identified the monoligand complexes MC_2H_4 for all the three metals, but the bi- and triligands were identified only with copper.[8] The more recent IR and Raman study of Merle-Mejean et al.[4] is not in complete agreement with the previous analysis: In contrast with McIntosh et al.,[17] these authors did not find any evidence for the monoligand complexes CuC_2H_4 and AgC_2H_4 in pure ethylene.

Up to now, only few theoretical investigations are available on some of these complexes. Xα calculations performed by McIntosh et al.[17] on the MC_2H_4 (M = Cu, Ag, Au) series failed in describing the observed optical spectrum. RHF calculations performed by Cohen and Basch[18] on the $Ag(C_2H_4)_{1,2}$ complexes did not give any evidence for bound states correlated to $Ag(d^{10}s^1)$. The CuC_2H_4 complex has been investigated through RHF calculations[19,20] and CI calculations that were discussed in detail in an earlier paper.[21]

The latter work was performed with canonical delocalized SCF MO's and concluded that the ground state was a π complex (C_{2v}) while the σ complex (C_s) was found to be higher in energy. Moreover, while the excited states of CuC_2H_4 were found to be chemically bound, the ground state was to be regarded as weakly bound (not bound at the RHF level) due to van der Waals interactions only.

It is well-known that the calculation of intermolecular forces within the supersystem approach with delocalized MO's is very tedious. Indeed, the configurations in the CI cannot be assigned a local character, and dispersion contributions cannot be separated from other physical effects (such as the variation of intrasystem correlation, polarization, charge-transfer contributions) or basis set superposition error. Dispersion contributions are generally much smaller than the other terms (particularly the intrasystem correlation), and any error on the extra terms may turn into unreliable results concerning the van der Waals bonding. It should be stressed that the position of the van der Waals minimum is

(1) See, for example: Parker, S. F.; Peden, C. H. F.; Barrett, P. H.; Pearson, R. G. *Inorg. Chem.* **1983**, *22*, 2813.
(2) For a review see: Zoellner, R. W.; Klabunde, K. J. *Chem. Rev.* **1984**, *84*, 545.
(3) Manceron, L.; Andrews, L. *J. Am. Chem. Soc.* **1985**, *107*, 563.
(4) Merle-MeJean, Th.; Boucharеb, S.; Tranquille, M. *J. Phys. Chem.* **1989**, *93*, 1197.
(5) Huber, H.; Ozin, G. A.; Power, W. J. *Inorg. Chem.* **1977**, *16*, 979.
(6) Hanlan, A. J. L.; Ozin, G. A.; Power, W. J. *Inorg. Chem.* **1978**, *17*, 3648.
(7) Ozin, G. A.; Power, W. J. *Inorg. Chem.* **1978**, *17*, 2836.
(8) Ozin, G. A.; Huber, H.; McIntosh, D. *Inorg. Chem.* **1977**, *16*, 3070.
(9) Grinter, R.; Stotesbury, S. J. *J. Mol. Struct.* **1982**, *80*, 125.
(10) Kasai, P. H. *J. Am. Chem. Soc.* **1982**, *104*, 1165.
(11) Kasai, P. H. *J. Phys. Chem.* **1982**, *86*, 3684.
(12) Chenier, J. H. B.; Howard, J. A.; Mile, B.; Sutcliffe, R. *J. Am. Chem. Soc.* **1983**, *105*, 788.
(13) Howard, J. A.; Sutcliffe, R.; Tse, J. S.; Mile, B. *Organometallics* **1984**, *3*, 859.
(14) Kasai, P. H. *J. Am. Chem. Soc.* **1984**, *106*, 3069.
(15) Kasai, P. H.; McLeod, D., Jr.; Watanabe, T. *J. Am. Chem. Soc.* **1980**, *102*, 179.
(16) Kasai, P. H. *J. Am. Chem. Soc.* **1983**, *105*, 6704.
(17) McIntosh, D. F.; Ozin, G. A.; Messmer, R. P. *Inorg. Chem.* **1980**, *19*, 3321.
(18) Cohen, D.; Basch, H. *J. Am. Chem. Soc.* **1983**, *105*, 6980.
(19) Itoh, H.; Kunz, A. B. *Chem. Phys. Lett.* **1979**, *66*, 531.
(20) Kelber, J. A.; Harrah, L. A.; Jennison, D. R. *J. Organomet. Chem.* **1980**, *199*, 281.
(21) Nicolas, G.; Barthelat, J. C. *J. Phys. Chem.* **1986**, *90*, 2870.

0002-7863/90/1512-5410$02.50/0

Table I. Pseudopotential Parameters for the Cu, Ag, and Au Atoms, $W_l(r) = e^{-\alpha r^2}\sum_i C_i r^{n_i}$

atom	l	α	C_i	n_i
Cu[a]	0	2.696 56	13.618	−1
			−24.624	0
			71.246	2
	1	0.596 40	0.129 38	−2
			7.869 4	−1
			−2.914 6	0
	2	1.464 56	−0.835 37	−2
			−3.220 6	−1
			6.793 1	1
			−5.570 1	2
Ag[b]	0	0.571 96	13.667 75	−1
			−2.891 33	2
			0.302 31	4
	1	1.098 07	21.145 16	0
	2	1.538 86	4.785 53	−2
			−17.187 29	0
			5.844 91	1
Au[b]	0	0.680 287	12.052 340	−1
			−0.952 243	2
	1	0.886 420	15.022 215	0
	2	1.958 924	1.303 018	−2
			27.173 962	0
			−35.796 947	1

[a] Reference 25. [b] Reference 26.

important if one wants to assign vertical transitions in the absorption spectrum.

In the present paper, we undertake a systematic theoretical study of the π-type complexes of the series MC_2H_4 (M = Cu, Ag, Au). This study includes RHF calculations and correlation treatment similar to that used in our previous work on CuC_2H_4. In addition, in order to provide realistic results on the bonding in the ground-state complexes, localized orbitals are used in the present work.

The previous study[21] on CuC_2H_4 showed that the attractive states correlated with the $d^{10}p^1$ atomic configuration of the metal could be treated independantly of the repulsive states, dissociating into the low-lying d^9s^2 configuration, at least at short distances, where the $d^{10}p^1$ states are bound. This is why the d^9s^2 configurations were not explicitely considered in the present calculations.

The ethylene moiety is expected to be weakly perturbed when complexing with the metal in the ground state. The relaxation of ethylene was indeed found to be rather negligible in our previous work on CuC_2H_4,[21] since the H_2C groups were found to be distorted out of plane by 3° and the CC bond length was found to be increased by 0.03 Å. Similar small geometry changes (2° out of plane and 0.02 Å CC bond length increasing) were also observed by Upton and Goddard[22] for ethylene in NiC_2H_4 π-coordinated complexes bound by as much as 14 kcal·mol^{-1}. In all our calculations the ethylene unit is then kept planar in the D_{2h} symmetry with the following geometry: R_{C-C} = 1.338 Å, R_{C-H} = 1.083 Å, and ∠HCH = 116.3°, optimized in our previous work.[21] The ethylene fragment lies in the $x0y$ plane, the C–C bond along the $0y$ axis, and the metal atom is on the $0z$ axis.

The methodology, emphasizing the localization process and the specific estimation of the dispersion contributions, is detailed in section II. Results on the π complexes involving a $d^{10}s^1$ metal are given in section III. The properties of the ground states are determined and discussed with respect to experimental data. The potential curves for the excited states dissociating into $d^{10}p^1$ configurations are given in section IV. The results concerning the optical spectra are given and discussed in the same section.

II. Methodological Details

Pseudopotentials and Basis Set. All the electrons of ethylene are explicitely considered, while the metal atoms are treated as 11-electron systems replacing the Ar-, Kr-, and Xe-like cores for Cu, Ag, and Au respectively, by nonempirical pseudopotentials of the Durand and Barthelat type,[23] including average relativistic effects.[24] Calculations are performed with Gaussian basis sets. The exponents and contraction coefficients of the basis sets and the pseudopotential parameters are given in Tables I and II, respectively.

Table II. Gaussian Atomic Basis Sets

atom	orbital	exponent	coefficient
C	s	3047.52	0.001 826
		456.424	0.014 057
		103.653	0.068 757
		29.225 8	0.230 422
		9.348 63	0.468 463
		3.189 04	0.362 780
		3.664 980	−0.747 384
		0.770 545	0.712 661
		0.195 857	1.0
	p	3.664 980	0.236 460
		0.770 545	0.860 619
		0.195 857	1.0
	s	13.247 876	0.019 255
		2.003 127	0.134 420
		0.455 867	0.469 565
		0.124 695	1.0
Cu	s	0.6540	1
		0.1102	1
		0.0376	1
	p	0.1914	0.379 9
		0.0776	0.508 5
		0.0316	0.221 9
		0.012	1.0
	d	28.87	0.069 8
		7.272 7	0.296 5
		2.356	0.479 4
		0.656 9	0.433 8
		0.12	0.129 9
Ag	s	0.513 364	1.0
		0.105 987	1.0
		0.027 494	1.0
	p	0.226 33	0.367 650
		0.071 235	0.611 257
		0.029 285	0.192 997
	d	31.007 447	−0.001 246
		10.575 429	−0.018 59
		2.155 256	0.402 42
		0.818 955	0.512 477
		0.256 272	0.298 606
Au	s	0.474 384	−0.494 389
		0.241 266	0.510 559
		0.073 698	1.0
		0.027 905	1.0
	p	0.862 067	−0.061 273
		0.178 199	0.560 434
		0.057 409	1.0
	d	3.486 256	−0.071 87
		2.034 844	0.252 407
		0.982 046	0.435 987
		0.420 003	0.372 158
		0.170 287	1.0
		0.073 422	1.0

Localized Molecular Orbitals. To make easier the analysis and provide a consistent description of the complex regarding the separated fragments, we have determined a set of localized MO's that keep as much as possible the valence character of the composing fragments. The use of a localized orbital makes possible (i) a partitioning of the energy into different physical contributions, (ii) a specific treatment of intermolecular dispersion forces, and (iii) a consistent and continuous treatment of correlation (truncation of the CI basis). On the other hand, the use of valence virtual orbitals improve the convergency of the CI process.[25,26]

(22) Upton, Th. H.; Goddard, W. A. *J. Am. Chem. Soc.* **1978**, *100*, 321.

(23) Durand, Ph.; Barthelat, J. C. *Theor. Chim. Acta* **1975**, *38*, 283. Barthelat, J. C.; Durand, Ph. *Gazz. Chim. Ital.* **1978**, *108*, 225.

(24) Barthelat, J. C.; Pelissier, M.; Durand, Ph. *Phys. Rev. A* **1980**, *21*, 1773.

(25) Pelissier, M. *J. Chem. Phys.* **1981**, *75*, 775.

Since we are interested essentialy in the states dissociating into ethylene + $M(d^{10}s^1/d^{10}p^1)$, we will first consider Mo's (f_i) that will be classified as follows: the two core orbitals of C_2H_4 correlated to the 1s carbone core AO's; the six occupied orbitals of C_2H_4 that are obtained for the ethylene fragment through a RHF closed-shell calculation; the six virtual orbitals of C_2H_4 that keep a valence character and cannot be the six lowest virtual MO's of the RHF calculation, since the valence character in the virtual subspace is spread over all the virtual MO's (therefore, in order to obtain valence virtual orbitals with the π^*- or the σ^*-ethylenic character, we used the hybridized atomic orbitals procedure (HAO) provided by Illas et al.;[25] the ns singly occupied orbital of the metal in its ground state; the np first excited orbital of the metal that is obviously necessary in order to describe the states dissociating into $M(d^{10}p^1)$ and considered here as part of the valence space; all the complementary virtual orbitals resulting from the calculation of the fragments in nonminimal basis sets.

An open-shell restricted Hartree–Fock calculation on MC_2H_4 was first performed, providing occupied (Φ_i) and virtual (Φ_i^*) orbitals for the complex. The two innermost MO's (Φ'_i) correspond to the 1s carbon core orbitals and were kept unchanged. The localization procedure was performed separately in the occupied subspace and the virtual subspace. We define

$$P = \sum_{i=3}^{14} |\Phi_i\rangle\langle\Phi_i|$$

as the projector onto the occupied subspace of the complex (the carbon core orbitals excepted) and

$$Q = \sum_{i\geq 15} |\Phi_i^*\rangle\langle\Phi_i^*|$$

as the projector onto the virtual subspace.

Localization in the occupied subspace was obtained by considering the projection $P|f_i\rangle$ of the occupied orbitals of the fragments (f_i = $2a_g$, $2a_u$, $1b_{3u}$, $3a_g$, $1b_{2g}$, and $1b_{2u}$ for ethylene, ns for the metal) and then orthogonalizing symmetrically the projections through the Löwdin $S^{-1/2}$ transform. In the same way, localization in the virtual subspace was performed by considering the projections $Q|f_i^*\rangle$ of the valence virtual orbitals of the fragments (f_i^* = $1b_{3g}$, $2b_{3u}$, $4a_g$, $3a_u$, $4a_u$, and $2b_{2g}$ for ethylene, np for the metal). The orthonormalization process, however, was carried on by privilegiating the np projection. The projections of ethylene MO's were orthogonalized to the metal orbitals, and an $S^{-1/2}$ transform was carried on afterward in order to orthonormalize them into one another. Finally, the virtual space was complemented by projecting and orthonormalizing the nonvalence virtual orbitals of the fragments, the redundant MO's being eliminated. This provides a set of localized occupied (φ_i^*) and virtual (φ_i) orbitals.

Treatment of the Ground State. In order to study specifically the $^2A_1$ ($d^{10}s^1$) ground state, a rather thorough study was carried on; indeed, the characterization of the equilibrium geometries will enable us to discuss better the vertical absorption spectrum in section IV.

In a second-order Møller-Plesset treatment over a single RHF reference, the total energy is given by

$$E(R) = E_{RHF}(R) + \epsilon_s^{(2)}(R) + \epsilon_D^{(2)}(R) \qquad (1)$$

R is the interfragment distance. E_{RHF} includes the Coulomb, exchange, polarization, and charge-transfer contributions.[29] The second term $\epsilon_s^{(2)}$ is the second-order contribution due to single excitations

$$\epsilon_s^{(2)} = \sum_{i,j^*} \frac{|\langle\varphi_i|F|\varphi_j^*\rangle|_2}{e_i - e_{j^*}}$$

The denominators refer to the one-electron energies $e_i = \langle\varphi_i|F|\varphi_i\rangle$. $\epsilon_s^{(2)}$ vanishes for closed-shell systems (due to Brillouin theorem)

(26) Barthelat, J. C. Private communication.
(27) Illas, F.; Merchan, M.; Pelissier, M.; Malrieu, J. P. *Chem. Phys.* **1986**, *107*, 361.
(28) Chambaud, G.; Gerard-Ain, M.; Kassab, E.; Levy B.; Pernot, P. *Chem. Phys.* **1984**, *90*, 271.
(29) Morokuma, K. *J. Chem. Phys.* **1971**, *55*, 1236.

Table III. Electric Dipole Polarizabilities (α, au^3) and Ionization Potentials (IP, eV) of Cu, Ag, Au, and C_2H_4

	Cu	Ag	Au	C_2H_4
α (accurate value)	61[a]	84[a]	88[a]	28[b]
α (present work)	58	75	48	6
IP[c]	7.72	7.57	9.22	10.5

[a] Reference 36. [b] Reference 37. [c] Reference 38.

and accounts for spin polarization, hereafter called $\epsilon_{spin}^{(2)}$ for open-shell systems as studied here. The remaining term $\epsilon_D^{(2)}$ is the second-order contribution due to double excitations

$$\epsilon_D^{(2)} = \sum_{i,j,k^*,l^*} \frac{\left|\left\langle \varphi_i(1)\ \varphi_j(2)\left|\frac{1}{r_{12}}\right|\varphi_k^*(1)\ \varphi_l^*(2)\right\rangle\right|^2}{e_i + e_j - e_k^* - e_l^*}$$

Since localized orbitals are used, $\epsilon_D^{(2)}$ can be partitioned into intra- and intersystem correlation terms $\epsilon_{intra}^{(2)}$ and $\epsilon_{disp}^{(2)}$, respectively. $\epsilon_{intra}^{(2)}$ is generated by double excitations from orbitals localized on the same fragment. $\epsilon_{disp}^{(2)}$ is generated by double excitations from orbitals localized on different fragments, and it typically corresponds to the dispersion energy. These terms have the same physical content (although they are not strictly identical) to the equivalent terms obtained in application of the London theory[30,31] with nonorthogonal wave functions. The total energy may then be written[32]

$$E(R) = E_{RHF}(R) + \epsilon_{spin}^{(2)}(R) + \epsilon_{intra}^{(2)}(R) + \epsilon_{disp}^{(2)}(R) \qquad (2)$$

The interaction energy ΔE can be defined as the difference between the total energy $E(R)$ and the sum of the isolated fragments energies $E(\infty)$ (supermolecule approach), e.g.,

$$\Delta E = E(R) - E(\infty) = \Delta E_{RHF} + \Delta\epsilon_{spin}^{(2)} + \Delta\epsilon_{intra}^{(2)} + \epsilon_{disp}^{(2)} \qquad (3)$$

with $\epsilon_{disp}^{(2)}(\infty) = 0$. In the case of weakly interacting fragments, the accurate evaluation of (3) is known to be rather tedious[33-35] due to the following considerations.

(i) The intrasystem correlation $\epsilon_{intra}^{(2)}$ is much larger than the dispersion term $\epsilon_{disp}^{(2)}$ while the corresponding interaction term $\Delta\epsilon_{intra}^{(2)}$ is usually much weaker.[34] A small difference between two independantly calculated large terms may become nonsignificant. Consequently any errors in the $\Delta\epsilon_{intra}^{(L)}$ term are likely to mask the dispersion term, which, although a small term, provides the main contribution to the binding energy.

(ii) The calculation of the dispersion energy requires very extensive basis sets, accounting for accurate polarizabilities of the separate fragments.

(iii) The basis set superposition errors (BSSE) may be of the same order of magnitude as the physical interactions.

In order to overcome those difficulties, we worked as follows:

(a) The intracorrelation $\epsilon_{intra}^{(2)}$ was supposed to have a negligible variation with the interfragment distance R. This assumption is commonly used when treating the interaction of closed-shell

(30) Heitler, W.; London, F. *Z. Phys.* **1927**, *44*, 1346. Eisenchitz, R.; London, F. *Z. Phys.* **1936**, *60*, 491. London, F. *Trans. Faraday Soc.* **1937**, *33*, 8.
(31) Claverie, P. In Intermolecular Interaction. *Diatomics to Polymers*; Pullmann, B., Ed.; John Wiley: New York, 1978.
(32) Daudey, J. P.; Claverie, P.; Malrieu, J. P. *Int. J. Quantum Chem.* **1974**, *8*, 1. Daudey, J. P.; Malrieu, J. P.; Rojas, O. *Int. J. Quantum Chem.* **1974**, *8*, 17. Spiegelmann, F.; Malrieu, J. P. *Mol. Phys.* **1980**, *40*, 1273.
(33) McLaughlin, D. R.; Schaeffer, H. F., III. *Chem. Phys. Lett.* **1971**, *12*, 244. Toennies, J. P. *Chem. Phys. Lett.* **1973**, *20*, 283. Stevens, W. J.; Wahl, A. C. *Phys. Rev. A* **1971**, *4*, 825. Ahlrichs, R.; Penco, R.; Scoles, G. *Chem. Phys.* **1977**, *19*, 119. See also: Hepburn, J.; Scoles, G.; Penco, R. *Chem.* Krauss, M.; Neumann, D. B. *J. Chem. Phys.* **1979**, *71*, 107. Krauss, M.; Neumann, D. B.; Stevens, W. J. *Chem. Phys. Lett.* **1979**, *66*, 29. Krauss, M.; Neumann, D. B.; Stevens, W. J. *Chem. Phys. Lett.* **1980**, *71*, 500.
(34) Liu, B.; McLean, A. D. *J. Chem. Phys.* **1973**, *59*, 4557.
(35) Boys, S. F.; Bernardi, F. *Mol. Phys.* **1970**, *19*, 553.
(36) Fraga, S.; Karwowski, J.; Saxena, K. M. S. *Handbook of Atomic Data*; Elsevier Scientific Publishing Co.: Amsterdam, 1976.
(37) Amos, R. D.; Williams, J. H. *Chem. Phys. Lett.* **1979**, *66*, 471.
(38) *Handbook of Chemistry and Physics*; 52nd ed.; The Chemical Rubber CO.: Cleveland, Ohio, 1971–1972.

systems; the energy is often assumed to be reasonably well accounted for by the sum of the SCF interaction energy and a multipolar expansion of the dispersion energy.[33] With the use of the same assumption in our case, and also considering the variation of the spin polarization contribution, the interaction energy reads

$$\Delta E = \Delta E_{RHF} + \Delta\epsilon_{spin}^{(2)} + \epsilon_{disp}^{(2)} \quad (4)$$

(b) The dispersion energy $\epsilon_{disp}^{(2)}$—or intersystem correlation—was easily computed with use of the set of localized MO's determined in the previous paragraph. However, this term is expected to be underestimated due to the electric dipole polarizabilities obtained for the separate fragments at the RHF level in the present basis. Their values are compared in Table III with more accurate ones. The main difference occurs for the ethylene fragment. In order to provide a realistic account of the dispersion contribution, $\epsilon_{disp}^{(2)}$ was scaled at $R = 15a_0$ with respect to the approximate London formula

$$\epsilon_{disp}^{London} = -\frac{3}{2}\frac{I_A I_B}{I_A + I_B}\frac{\alpha_A \alpha_B}{R^6}$$

where α_A and α_B are the electric dipole polarizabilities of the separate fragments A and B and I_A and I_B are their ionization potentials. The scaling factors were found to be 3.8, 4, and 4.6 for CuC_2H_4, AgC_2H_4, and AuC_2H_4, respectively. The $\epsilon_{disp}^{(2)}$ values were then corrected by the specific factors for all the interfragment distances $R < 15a_0$.

(c) Since we have treated specifically the dispersion term $\epsilon_{disp}^{(2)}$, the BSSE only affects the RHF interaction energy and the spin polarization term in expression 4. It was estimated by using the counterpoise correction,[35] i.e., computing the variation of $E_{RHF} + \epsilon_{spin}^{(2)}$ for each fragment A and B due to the presence of the partner orbitals at each distance R, e.g., in the total basis set {A}U{B} of the complex. In the case of the RHF energy the correction is the following

$$\delta_{BSSE}^{RHF} = E_A^{RHF}\{A\} - E_A^{RHF}(\{A\}U\{B\}) + E_B^{RHF}\{B\} - E_B^{RHF}(\{A\}U\{B\})$$

An identical expression is readily obtained for the spin polarization correction δ_{BSSE}^{spin}. Accounting for the total BSSE correction

$$\delta_{BSSE}(R) = \delta_{BSSE}^{RHF}(R) + \delta_{BSSE}^{spin}(R)$$

the interaction energy is finally given by

$$\Delta E = \Delta E_{RHF} + \Delta\epsilon_{spin}^{(2)} + \epsilon_{disp}^{(2)} + \delta_{BSSE} \quad (5)$$

Treatment of the Excited States. The CI process used is a second-order multireference (MR) perturbative treatment in the Møller-Plesset scheme (CIPSI algorithm[39]) as in our previous work. In $^2A_1$ symmetry, the zeroth-order states are provided by diagonalization of a basic MR subspace including two configurations, i.e., the RHF configuration corresponding to the ground state of the MC_2H_4 complex ($M(d^{10}s^1)$, for the sake of orthogonality) and the second configuration related to the first excited state of same symmetry ($M(d^{10}p_z^1)$). As concerns the total energy of the first $^2A_1$ root (ground state), the present treatment does not yield significant differences with respect to the basic MP2 result with only one reference (eq 2), indicating that the two $^2A_1$ states are very weakly coupled.

For $^2B_1$ and $^2B_2$ species the perturbed subspace included only the single configurations related to the metal excited states, $d^{10}p_x^1$ and $d^{10}p_y^1$, respectively, and the CI is then an ordinary Møller-Plesset second-order treatment. It was checked that taking into account larger MRCI spaces does not change significantly the results.

The excited states are affected by the same defects as those mentioned for the ground state (BSSE and underestimation of the polarizability of ethylene essentially). Those defects can be estimated by the difference between the MRCI-MP2 present results for the $^2A_1$ ($d^{10}s^1$) ground state and those found in the previous section (eq 5). Thus, all excited states were lowered by the same R-dependant shift corresponding to this difference. Indeed, the error may be supposed to be transferable as long as it is essentially attributed to ethylene.

(39) Huron, B.; Malrieu, J. P.; Rancurel, P. *J. Chem. Phys.* **1973**, *58*, 5745.

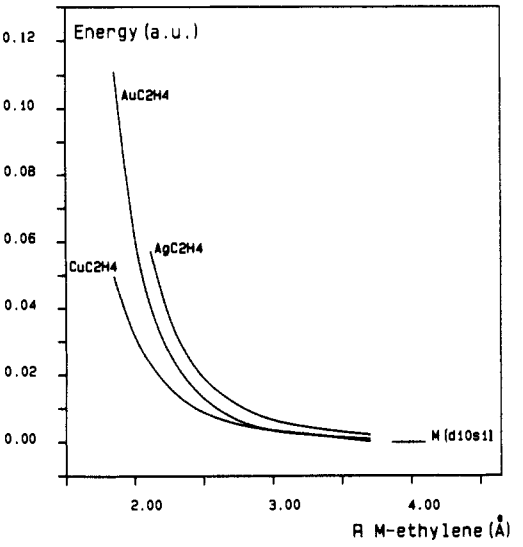

Figure 1. RHF potential energy curves of the $^2A_1(d^{10}s^1)$ ground states of CuC_2H_4, AgC_2H_4, and AuC_2H_4. Energies are relative to the $d^{10}s^1$ dissociation for all systems.

Table IV. Equilibrium Distances and Binding Energies for the Low-Lying States of the CuC_2H_4, AgC_2H_4, and AuC_2H_4 Complexes

	CuC_2H_4		AgC_2H_4		AuC_2H_4	
state	R_e, Å	D_e, kcal·mol^{-1}	R_e, Å	D_e, kcal·mol^{-1}	R_e, Å	D_e, kcal·mol^{-1}
$^2A_1(p_z^1)$	2.17	14				
$^2B_1(p_x^1)$	2.22	27	2.49	19	2.17	42
$^2B_2(p_y^1)$	2.12	33	2.43	25	2.17	66
$^2A_1(s^1)$	2.65	3	3.02	2	2.43	12

III. Ground State

At the RHF level, the metal($d^{10}s^1$)–ethylene interaction is found to be repulsive for the three complexes (see Figure 1) and no real chemical bond is established. The ordering of the repulsive character is $AgC_2H_4 > AuC_2H_4 > CuC_2H_4$. The single occupied molecular orbital ($7a_1$ MO) always appears to present a nodal plane between the C–C axis and the metal (see Figure 2).

The potential curves obtained from the expression (5) of the interaction energy are shown in Figure 3. All three complexes, CuC_2H_4, AgC_2H_4, and AuC_2H_4, are seen to be bound, essentially due to the dispersion contribution and, for a smaller part, to the spin polarization that tends to increase at smaller distances. The equilibrium distances and dissociation energies are reported in Table IV. The gold complex is the most strongly bound with the shortest equilibrium distance. The copper and silver complexes are more weakly bound, and at short interfragment distance ($R < 6a_0$) the AgC_2H_4 complex is the most repulsive. This situation is to be related to the relativistic effects that completely invert the mean radius of the atomic ns orbital with respect to the ordering of the periodic table (1.74, 1.82, and 1.62 Å for Cu,[40] Ag,[26] and Au,[26] respectively). The same trend for equilibrium distances is often observed when noble-metal atoms are engaged in different types of bonds.[41,42] In recent relativistic calculations on AgH_2 and AuH_2, Balasubramanian and Liao[43] also found the $^2B_2$ state of the AuH_2 system to be more stable, with the Au–H bond length smaller than the Ag–H bond length (AuH_2 and AgH_2 present, however, real chemical bondings, unlike the complexes

(40) Pelissier, M. Thesis, Université de Toulouse, France, 1980.
(41) Pauling, L. *The Nature of Chemical bond*; Cornell University Press: New York, 1960.
(42) Walch, S. P.; Bauschlicher, C. W., Jr.; Langhoff, S. R. *J. Chem. Phys.* **1986**, *85*, 5900.
(43) Balasubramanian, K.; Liao, M. Z. *J. Phys. Chem.* **1989**, *93*, 89.

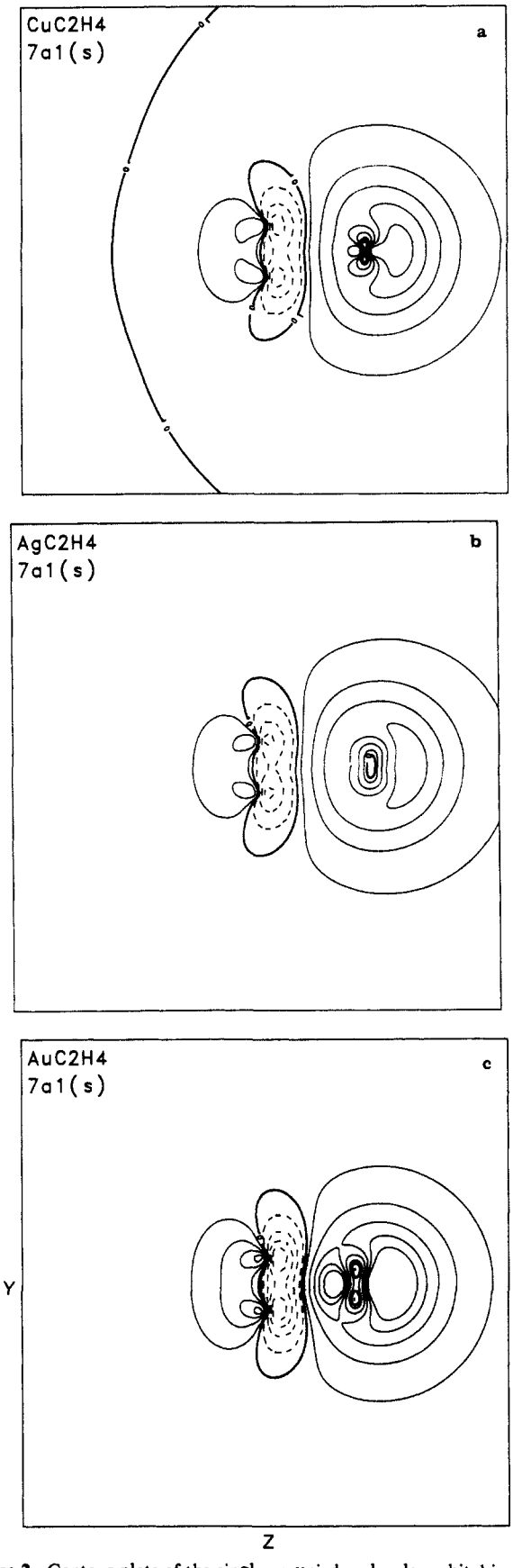

Figure 2. Contour plots of the single occupied molecular orbital in the $^2A_1(s^1)$ ground states of CuC_2H_4, AgC_2H_4, and AuC_2H_4. Nodal lines are bold. The sides of plots a, b, c are 13 Å long.

under study in the present section).

The Mulliken total gross population analysis was computed with the one-particle density matrix for the ground-state RHF determinant perturbed up to the first order. The common feature

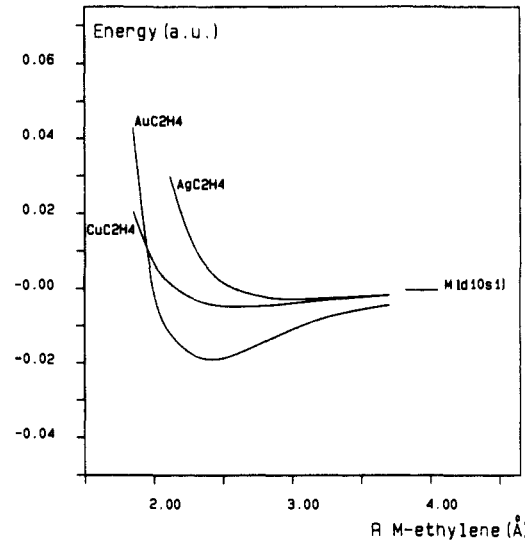

Figure 3. Potential energy curves of the $^2A_1(d^{10}s^1)$ ground states of CuC_2H_4, AgC_2H_4, and AuC_2H_4. Energies are relative to the $d^{10}s^1$ dissociation for all systems.

Table V. Gross Atomic Population for CuC_2H_4, AgC_2H_4, AuC_2H_4, and Free Ethylene in Their Ground States

	atom	d	s	p	total
CuC_2H_4	Cu	9.99	1.01	0.12	11.13
	C		3.34	2.97	6.31
	H		0.81		0.81
AgC_2H_4	Ag	9.99	1.02	0.08	11.09
	C		3.33	2.99	6.31
	H		0.82		0.82
AuC_2H_4	Au	9.89	1.05	0.18	11.12
	C		3.36	2.98	6.34
	H		0.79		0.79
C_2H_4	C		3.31	2.99	6.30
	H		0.85		0.85

Table VI. Molecular Population Analysis in CuC_2H_4, AgC_2H_4, and AuC_2H_4 at the Ground-State Equilibrium Distance

		M			C		H
		d	s	p	s	p	s
CuC_2H_4	$2a_1(d_{z^2})$	1.00	0.00	0.00	0.00	0.00	0.00
	$6a_1(\pi)$	0.00	0.04	0.02	0.00	0.47	0.00
	$7a_1(s)^a$	0.00	0.93	0.06	0.00	0.01	0.00
	$2b_2(d_{yz})$	1.00	0	0.00	0.00	0.00	0.00
AgC_2H_4	$2a_1(d_{z^2})$	1.00	0.00	0.00	0.00	0.00	0.00
	$6a_1(\pi)$	0.00	0.02	0.01	0.00	0.48	0.00
	$7a_1(s)^a$	0.00	0.96	0.03	0.00	0.01	0.00
	$2b_2(d_{yz})$	1.00	0	0.00	0.00	0.00	0.00
AuC_2H_4	$2a_1(d_{z^2})$	0.96	0.04	0.00	0.00	0.00	0.00
	$6a_1(\pi)$	0.00	0.10	0.02	0.00	0.45	0.00
	$7a_1(s)^a$	0.03	0.81	0.11	0.00	0.03	0.00
	$2b_2(d_{yz})$	0.97	0	0.00	0.00	0.01	0.00

[a] $7a_1$ is the single occupied MO.

(Table V) is a small charge transfer from ethylene toward the metal (of the order of 0.1e). Analysis of the gross population per atomic shell shows that the p orbital tends to take benefit of this transfer with increasing occupation in the order Ag < Cu < Au. The population of the s shell is also increased but to a lesser extent. One may also notice that, for AuC_2H_4, the d shell is slightly depopulated while this effect is vanishing in the case of CuC_2H_4 and AgC_2H_4. If one examines the RHF MO's population in Table VI, it is noticed that the population of the p metal orbital is essentially due to direct s-p hybridization in the $7a_1$ orbital, which is correlated with the s metal orbital. However, this electron increase in the p orbital is also due to a small transfer from the π-ethylene orbital (6_1 MO). One can see that the $\pi \rightarrow$ s ligand $\rightarrow$ metal charge transfer is quite negligible for silver and becomes significant for the gold complex (0.20e in $6a_1$). The small de-

Table VII. Calculated and Experimental Energies (eV) of the $d^{10}s^1 \rightarrow d^{10}p^1$ Transition for Copper, Silver, and Gold Atoms

	Cu	Ag	Au
present work	3.95	3.50	4.59
experiment[a]	3.80	3.74	4.94

[a] Reference 46.

population of the d orbital in the AuC_2H_4 case is due partly to s-d_{z^2} mixing and partly to metal-ligand transfer, $d_{xz} \rightarrow \pi^*$. In no case are those transfers large enough to induce a real chemical stabilization of the complexes in their ground state. They probably help to reduce the repulsion between ethylene and the metal, especially in the AuC_2H_4 case.

Our conclusions for the ground state are thus different from the classical Dewar-Chatt-Duncanson[44] (DCD) scheme that explains the metal-olefin bonding as due to two dative interactions, one being the π(ligand) $\rightarrow$ s(metal) donation, the second one the d(metal) $\rightarrow \pi^*$(ligand) back-donation. The present results for AgC_2H_4 and AuC_2H_4, as well as those on CuC_2H_4, are consistent with similar results obtained by Upton and Goddard[22] or Bash et al.[45] on NiC_2H_4, who also found the donation and back-donation contributions to be rather weak. It has been shown in our previous work on CuC_2H_4[21] that these charge transfers remain rather poor even when relaxation (shown to be small) of the ethylene unit was taken into account. Ethylene relaxation may be more significant in AuC_2H_4, but it should not modify in a drastic way the nature of the interaction. (Note that, as previously mentioned, the three complexes are not bound at the RHF level, which indicates no strong chemical bond.)

ESR experiments by Kasai et al.[15,16] provide spectra for these complexes trapped in rare-gas matrices. The ESR spectra result from the interaction between the electron spin of the unpaired electron and the different nuclear spins in the presence of an external magnetic field. This interaction is measured by the magnitude of the hyperfine (hf) coupling tensor to the metal nuclei, which is supposed to be related to the distribution of the electron density on the nuclei. Kasai et al. observe that the hf coupling with the hydrogens is very weak for all systems, in agreement with our population analysis of the unfilled orbital ($7a_1$) in Table VI showing vanishing weights on hydrogens, all of them being less than 0.002. On the other hand, the examination of anisotropy properties of the hf tensor and comparison of the isotropic A_{iso} and anisotropic A_{disp} constants with those of single metal atoms trapped under the same conditions lead Kasai et al. to predict some significant s-p mixing in the case of AuC_2H_4 and CuC_2H_4, while the AgC_2H_4 signal is found to be identical with the atomic case. Calculations show not even a small hybridization pattern. Although participation of the p_z components in the single occupied MO ($7a_1$) is on the same order as predicted by Kasai (Au > Cu > Ag), its magnitude is very weak (see Table VI and Figure 2). Our conclusions are that the larger binding for AuC_2H_4, and to a less extent of CuC_2H_4 with respect to AgC_2H_4, should not be interpreted as due to hybridization, but as due essentially to dispersion forces.

IV. Excited States

The calculated atomic transitions corresponding to $d^{10}s^1 \rightarrow d^{10}p^1$ are shown in Table VII as compared to experimental transitions. The agreement is 4% for Cu, 6g for Ag, and 7% for Au. The excited-state potential curves have been shifted by the asymptotic error. They are given in Figures 4-6 with respect to the $^2A_1(s^1)$ ground state. Equilibrium distances and dissociation energies are listed in Table IV.

For all complexes, the ordering of the states is the same; i.e., $^2A_1(s^1) < {}^2B_2(p_y{}^1) < {}^2B_1(p_x{}^1) < {}^2A_1(p_z{}^1)$ in the whole distance range. The $^2B_2(p_y{}^1)$ and $^2B_1(p_x{}^1)$ are bound, while $^2A_1(p_z{}^1)$, weakly bound for CuC_2H_4, is found to be weakly repulsive in the case of AgC_2H_4 and AuC_2H_4. In contrast with the ground state, the two first excited states exhibit a real bonding, with shorter equilibrium distances for the whole series. However, the ordering of the binding energies is inchanged; i.e., $AuC_2H_4 > CuC_2H_4 >$

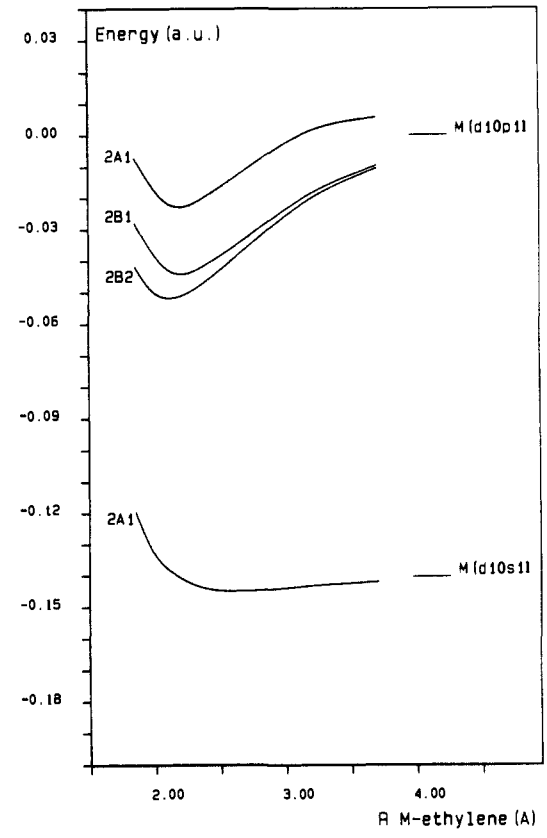

Figure 4. Potential energy curves of the lowest electronic states of the AgC_2H_4 complex. Energies are relative to the $4d^{10}5p^1$ dissociation.

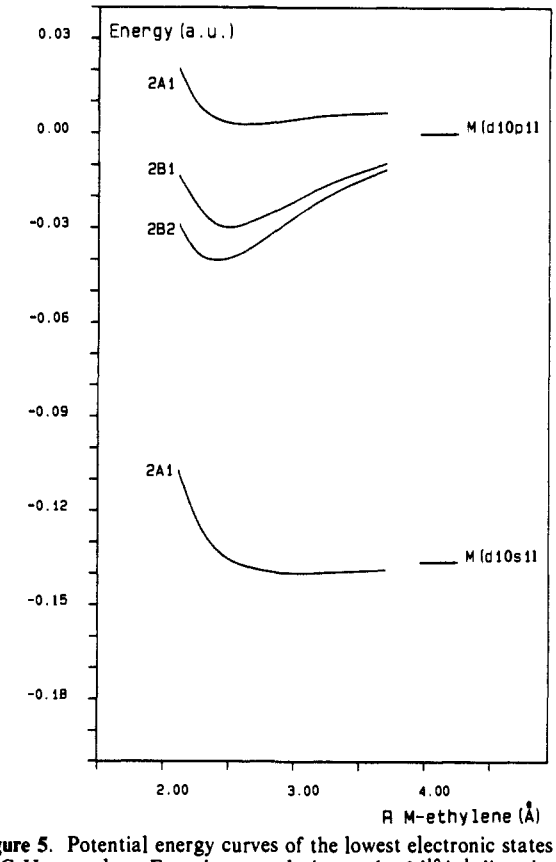

Figure 5. Potential energy curves of the lowest electronic states of the CuC_2H_4 complex. Energies are relative to the $3d^{10}4p^1$ dissociation.

(44) Dewar, M. J. S. *Bull. Soc. Chim. Fr.* **1951**, *18C*, 79. Chatt, J.; Duncanson, L. A. *J. Chem. Soc.* **1953**, 2939.
(45) Basch, H.; Newton, M. D.; Moskowitz, J. W. *J. Chem. Phys.* **1978**, *69*, 584.
(46) Moore, C. F. *Atomic Energy Levels, National Bureau of Standards Circular*; Department of Commerce: Washington, DC, 1971; No. 35.

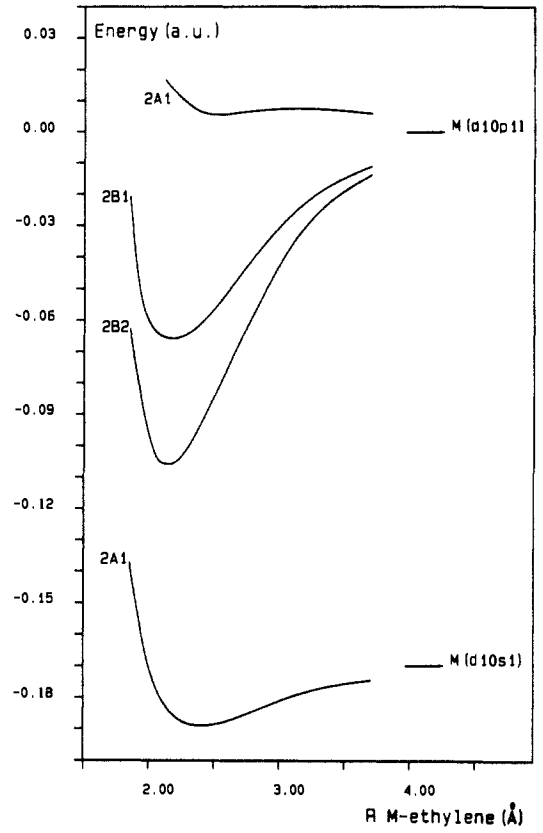

Figure 6. Potential energy curves of the lowest electronic states of the AuC_2H_4 complex. Energies are relative to the $5d^{10}6p^1$ dissociation.

Table VIII. Gross Atomic Population Analysis in the $^2B_1(p_x^1)$ and $^2B_2(p_y^1)$ States of CuC_2H_4, AgC_2H_4, and AuC_2H_4

	atom	state	d	s	p	total
CuC_2H_4	Cu	$^2B_1$	9.96	0.18	1.08	11.22
		$^2B_2$	9.96	0.18	1.05	11.19
	C	$^2B_1$		3.38	2.96	6.34
		$^2B_2$		3.38	2.97	6.35
	H	$^2B_1$		0.77		0.77
		$^2B_2$		0.78		0.78
AgC_2H_4	Ag	$^2B_1$	9.96	0.14	1.06	11.16
		$^2B_2$	9.96	0.14	0.97	11.07
	C	$^2B_1$		3.38	2.98	6.36
		$^2B_2$		3.38	3.02	6.39
	H	$^2B_1$		0.78		0.78
		$^2B_2$		0.79		0.79
AuC_2H_4	Au	$^2B_1$	9.79	0.41	1.08	11.28
		$^2B_2$	9.81	0.42	0.77	11.01
	C	$^2B_1$		3.40	2.95	6.35
		$^2B_2$		3.39	3.06	6.45
	H	$^2B_1$		0.75		0.75
		$^2B_2$		0.77		0.77

AgC_2H_4. One may notice that dissociation energies of the AuC_2H_4 states are about twice those of CuC_2H_4 or AgC_2H_4.

Nature of the Bonding. Gross populations for the excited states have been determined near their equilibrium distances, as was done for the ground state (Table VIII). One major feature is revealed by the population of the vacant s orbital of the metal, which is of same magnitude for $^2B_2$ and $^2B_1$ states. This s population turns out to be very important in the case of AuC_2H_4 ($\simeq$0.4e). A second interesting feature is the behavior of the d shell of the metal: The d population remains quasi-atomic in the case of CuC_2H_4 and AgC_2H_4, while a significant default ($\simeq$0.2e) is observed in the case of AuC_2H_4. The MO population (Table IX) shows clearly that the population of the s orbital is essentially due to a $\pi \rightarrow$ s donation (see $6a_1$ MO). In the case of gold, however, a non-negligible contribution is also due to d_{z^2}–s mixing, therefore depopulating the d shell ($2a_1$ MO, Table IX). Note that the depopulation of this d shell is also caused by a d $\rightarrow \pi^*$ back-donation ($2b_2$ MO, Table IX). The population of the p shell also exhibits a striking behavior. It is slightly increased in the case of the $^2B_2$ state for all complexes. In contrast, it tends to significantly diminish in the case of AuC_2H_4 in the $^2B_2$ state. The MO population analysis shows that this effect is caused by an electron transfer from the metal p_y orbital toward the ligand π^* orbital ($4b_2$, Table IX).

Table IX. Molecular Population Analysis in the $^2B_1(p_x^1)$ and $^2B_2(p_y^1)$ States of CuC_2H_4, AgC_2H_4, and AuC_2H_4

		M			C		H
		d	s	p	s	p	s
CuC_2H_4	$2a_1(d_{z^2})$	0.99	0.01	0.00	0.00	0.00	0.00
	$6a_1(\pi)$	0.00	0.06	0.02	0.00	0.46	0.00
	$3b_1(p_x)$	0	0	1.0	0	0.00	0.00
	$2b_2(d_{yz})$	0.97	0	0.00	0.00	0.01	0.00
	$4b_2(p_y)$	0.00	0	0.96	0.00	0.02	0.00
AgC_2H_4	$2a_1(d_{z^2})$	1.0	0.01	0.00	0.00	0.00	0.00
	$6a_1(\pi)$	0.00	0.05	0.00	0.00	0.48	0.00
	$3b_1(p_x)$	0	0	1.01	0	0.00	0.00
	$2b_2(d_{yz})$	0.99	0	0.00	0.00	0.01	0.00
	$4b_2(p_y)$	0.00	0	0.92	0.00	0.05	0.00
AuC_2H_4	$2a_1(d_{z^2})$	0.94	0.06	0.00	0.00	0.00	0.00
	$6a_1(\pi)$	0.00	0.13	0.01	0.00	0.43	0.00
	$3b_1(p_x)$	0	0	1.01	0	0.00	0.00
	$2b_2(d_{yz})$	0.93	0	0.00	0.01	0.03	0.00
	$4b_2(p_y)$	0.02	0	0.69	0.00	0.16	0.00

Thus, the stability of the excited complexes can be understood as follows. For CuC_2H_4 and AgC_2H_4, stabilization of both $^2B_1$ and $^2B_2$ states is ensured by a ligand $\rightarrow$ metal transfer of $\pi \rightarrow$ s type

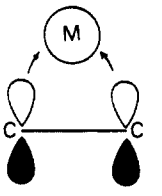

and not significant metal $\rightarrow$ ligand transfer appears. In particular in the $^2B_2$ state, the delocalization of the p unpaired electron toward the π^* MO remains very weak (see the $4b_2$ MO in table IX). This explains the weak stabilization of $^2B_2$ with respect to $^2B_1$, where the above delocalization is symmetry forbidden.

In the case of AuC_2H_4, the same features are observed, but they are considerably enhanced. In particular, the $\pi \rightarrow$ s donation is stronger ($6a_1$ MO, 0.27e) and the d $\rightarrow \pi^*$ back-donation

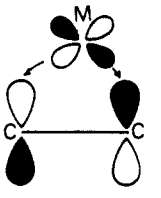

becomes significant ($2b_2$ MO, 0.11e), which explains the increased stabilization of both $^2B_2$ and $^2B_1$ states with respect to the other complexes. In addition to these transfers, in the $^2B_2$ case a significant metal $\rightarrow$ ligand transfer is obtained since the p_y single occupied orbital of the metal shows very strong delocalization toward the π^* orbital of ethylene ($4b_2$, 0.40e). This $p_y \rightarrow \pi^*$ transfer

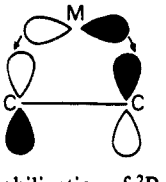

explains the important stabilization of $^2B_2$ in the case of AuC_2H_4. In this excited complex, the classical DCD scheme[40] reasonably

Table X. UV-Visible Spectra (Vertical Transitions) of the CuC_2H_4, AgC_2H_4, and AuC_2H_4 Complexes (eV)

	CuC_2H_4	AgC_2H_4	AuC_2H_4
$^2A_1(s^1) \rightarrow {}^2B_1(p_x^1)$	3.01 (3.25)[a]	3.27	3.81 (4.00)[a]
$^2A_1(s) \rightarrow {}^2B_2(p_y^1)$	2.88 (2.95)[a]	3.10	2.99 (3.09)[a]

[a] Experimental Values.[17]

accounts for the bonding.

The more important charge transfers observed from the d shell in the case of gold (d_{z^2}–s mixing and $d_{xy} \rightarrow \pi^*$ back-donation) can be related to the radial extension of the d orbitals (0.53, 0.73, and 0.84 Å for Cu,[40] Ag,[26] and Au,[26] respectively). The noticeable relativistic contractions of s and p orbitals in gold probably favor the $\pi \rightarrow$ s and the p $\rightarrow \pi^*$ charge transfers observed in AuC_2H_4 by decreasing repulsion between metal and ethylene. Figures 7–9 clearly illustrate the role played by the respective sizes of the p orbitals of the three metallic atoms. In particular, the differences observed for the $^2A_1(p_z)$ state in the series can be explained from Figure 9: In the case of AgC_2H_4 and AuC_2H_4 the more contracted character of the p metal orbital yields a nodal plane between the C–C axis of ethylene and the metal, which prevents any bonding. In CuC_2H_4, since the p copper orbital is more diffuse, no nodal plane appears between the interacting entities, thus favoring a bonding.

Relaxation of ethylene should be of importance in these excited states as it has been shown in our earlier work on CuC_2H_4.[21] However, as we are interested in the vertical transitions, we do not take it into account in the present work.

Spectra. The vertical transitions $^2A_1(s^1) \rightarrow {}^2B_2(p_y^1)$ and $^2A_1(s^1) \rightarrow {}^2B_1(p_x^1)$ are reported in Table X for the three complexes. These transitions are located in the visible and near-UV spectrum, and all appear to be red-shifted with respect to their values in the free atoms, due to the stabilities of the excited states and the weakly bound character of the ground state.

Infrared and optical spectra have been obtained by McIntosh et al.[17] for the three complexes trapped in an argon matrix. Each complex presents two absorption peaks in the visible–UV region. A satisfactory agreement (error <0.25 eV, $\simeq$5%) is observed between calculated and experimental transitions in the case of CuC_2H_4 and AuC_2H_4, as can be seen in Table X. In the case of AgC_2H_4, one of the transitions recorded by McIntosh et al. is strongly red-shifted (λ = 551 nm), while the other is strongly blue-shifted inside the UV region (λ = 270 nm), establishing a significant discontinuity in the series. This is not reproduced in our calculations.

One may, however, notice that some ambiguities subsist as concerns the IR identification of the different n–m stoichiometries possible for a $M_n(C_2H_4)_m$ complex, as was recently shown by an IR and Raman study of Merle-Mejean et al.[4] Thus, is it possible that the transitions observed by McIntosh on the silver complex belong to a highest stoichiometry complex as proposed by Merle-Mejean et al. Our results support this proposition, not only because of the disagreement observed on the transitions but also because of the very weak stability of the ground state of AgC_2H_4.

V. Conclusion

In their $^2A_1$ ground state, which dissociates into the metal $d^{10}s^1$ configuration, the complexes CuC_2H_4, AgC_2H_4, and AuC_2H_4 appear to be weakly bound. No bonding is obtained at the RHF level when BSSE is accounted for, and those complexes appear to be essentially stabilized by dispersion forces, as previously mentioned for CuC_2H_4. The electronic structures of the metal and ethylene fragments are weakly affected by the interaction, as illustrated by population analyses, and the unpaired electron remains localized in the external orbital of the metal. This description is consistent with analysis of these compounds as van der Waals compounds. The very small wells obtained for CuC_2H_4 and AgC_2H_4 could explain the difficulties to form the manifold 1:1 complex in some experiments.

Concerning the dissociation into the metal $d^{10}p^1$ configurations, only the $^2B_2$ and $^2B_1$ states give rise to chemically stable excited complexes for the whole series. The bonding can be analyzed in terms of the following charge-transfer processes:

(i) The ligand $\rightarrow$ metal $\pi \rightarrow$ s donation is equally present in the $^2B_1$ or $^2B_2$ states. This charge transfer appears to be of

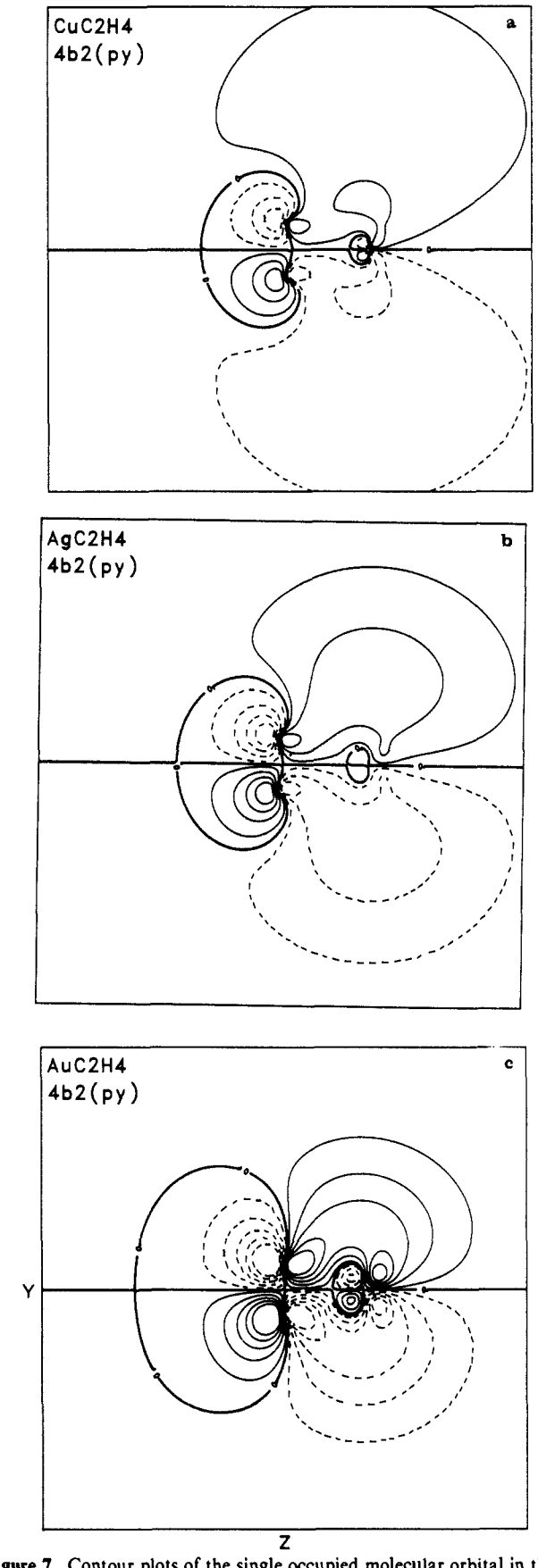

Figure 7. Contour plots of the single occupied molecular orbital in the $^2B_2(p_y^1)$ states of CuC_2H_4, AgC_2H_4, and AuC_2H_4. Nodal lines are bold. The sides of plots a, b, c are 13 Å long.

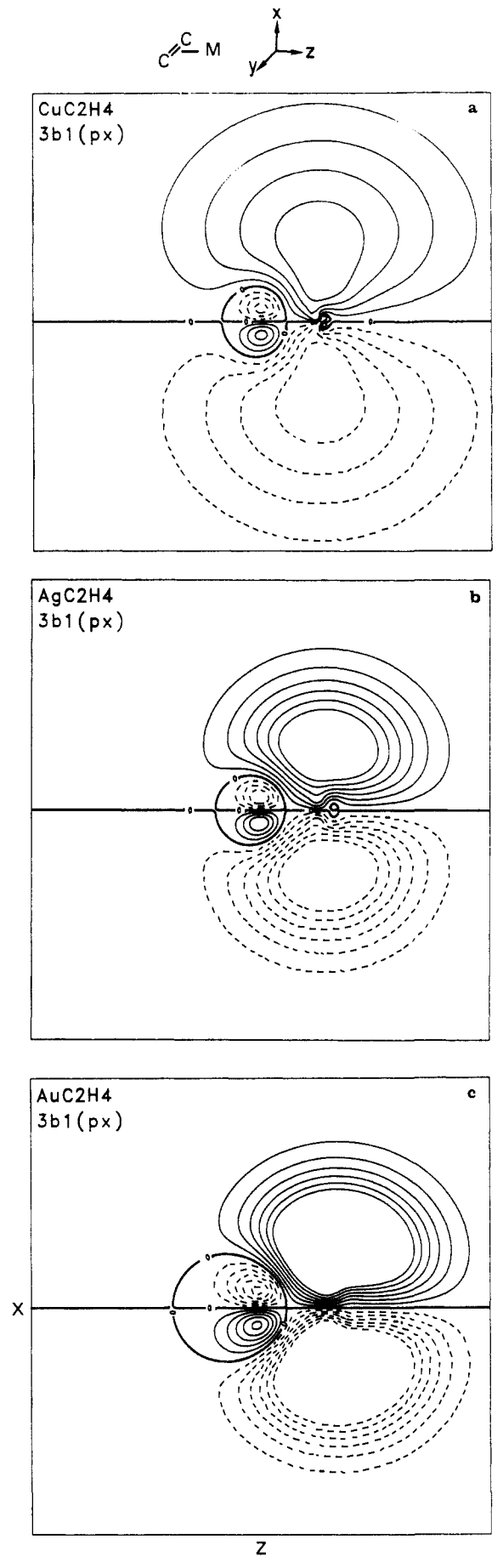

Figure 8. Contour plots of the single occupied molecular orbital in the $^2B_1(p_x^1)$ states of CuC_2H_4, AgC_2H_4, and AuC_2H_4. Nodal lines are bold. The sides of plots a, b, c are 13 Å long.

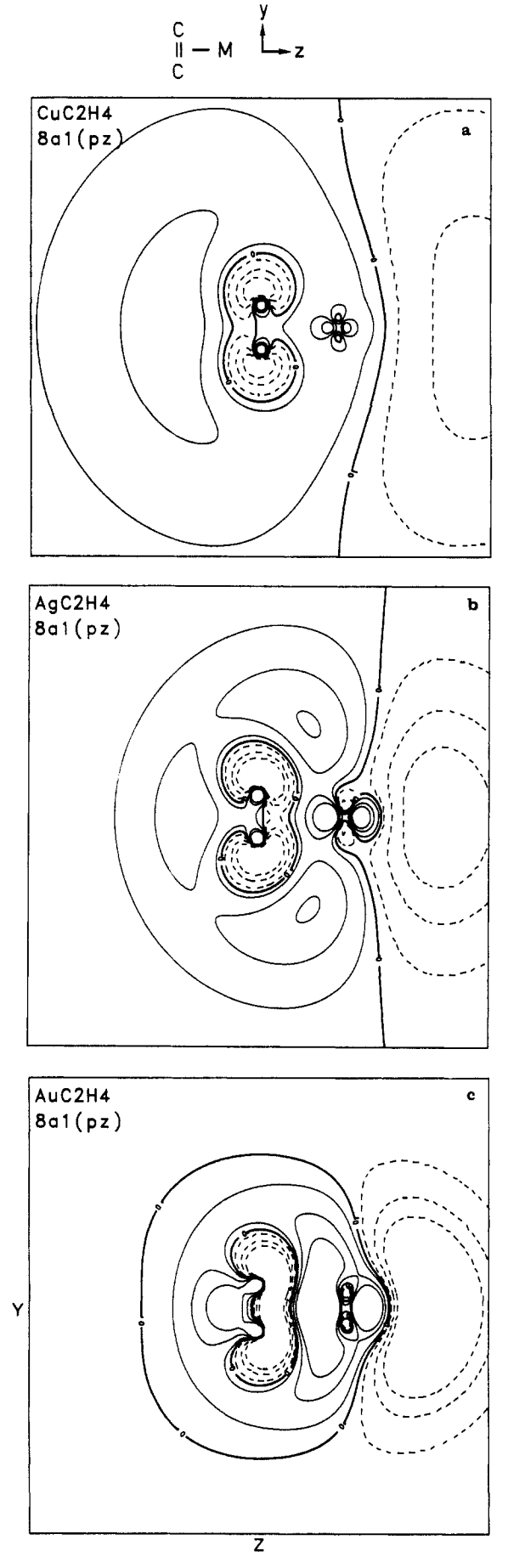

Figure 9. Contour plots of the single occupied molecular orbital in the $^2A_1(p_z^1)$ states of CuC_2H_4, AgC_2H_4, and $AuCH_4$. Nodal lines are bold. The sides of plots a, b, c are 13 Å long.

importance for the three complexes, but it is particularly enhanced in the case of AuC_2H_4.

(ii) The metal → ligand d → π^* back-donation is only significant for the $^2B_1$ and $^2B_2$ states of AuC_2H_4.

(iii) The metal → ligand p → π^* back-donation only occurs in the $^2B_2(p_y^1)$ state. This charge transfer is of weak importance in the CuC_2H_4 and AgC_2H_4 complexes while it is of the same magnitude as the π → s donation in the AuC_2H_4 complex.

From the study of the whole series, we can conclude that gold is the metal that shows the strongest interaction with ethylene, in either $d^{10}s^1$ or $d^{10}p^1$ configuration. Cu or Ag always present weaker interactions. This behavior is to be related to relativistic effects, which already affect the atomic properties in the series.

The vertical transitions determined in the present work are in reasonable agreement with the experiment spectra of McIntosh et al. for CuC_2H_4 and AuC_2H_4: Two lines were observed and can be assigned to transitions $^2A_1(s^1)$ → $^2B_2(p_y^1)$ and $^2A_1(s^1)$ → $^2B_1(p_x^1)$. Concerning AgC_2H_4, our calculation provides results between those of CuC_2H_4 and AuC_2H_4, in contradiction with the observations of McIntosh et al. who attribute to the AgC_2H_4 complex two lines strongly shifted (blue and red, respectively) with respect to the asymptotic transition. It should be checked whether the experimental spectra involving Ag atoms do correspond to the mononuclear 1:1 complex, or whether they might be related to higher stoichiometry or to polynuclear species.

Acknowledgment. We are very grateful to Dr G. Trinquier for carefully reading the manuscript and suggeting helpful comments.